Ab Initio MO Study of Selected Aluminum and Boron Chlorides and Fluorides: Comparison with ^{11}B NMR Spectra of a Tetrachloroborate Melt

STEPHEN D. WILLIAMS*
Department of Chemistry, Appalachian State University, Boone, North Carolina 28608

WARREN HARPER
Department of Chemistry, University of Kentucky, Lexington, Kentucky 40506

GLEB MAMANTOV and LOUIS J. TORTORELLI
Department of Chemistry, University of Tennessee, Knoxville, Tennessee 37996-1600

GEORGE SHANKLE
Department of Chemistry, Angelo State University, San Angelo, Texas 76909

Received 22 May, 1995; accepted 10 January, 1996

ABSTRACT

Molecular geometries were fully optimized for $AlCl_3$, $AlCl_4^-$, Al_2Cl_6, $Al_2Cl_7^-$, AlF_3, AlF_4^-, Al_2F_6, $Al_2F_7^-$, BCl_3, BCl_4^-, B_2Cl_6, $B_2Cl_7^-$, BF_3, BF_4^-, B_2F_6, and $B_2F_7^-$, as well as a few mixed halogen species, at the Hartree–Fock (HF) level, using basis sets from STO-3G to 6–311 + $G(d)$. In some cases geometries were also optimized at the MP2 level. Where possible, the computed geometries were compared to known structures from electron or X-ray diffraction. The agreement between these was quite good for the neutral species, and somewhat poorer for the anions. Vibrational frequencies were calculated for all species at the HF level with the largest basis set. The geometries were characterized as minima or transition structures. Various formation reaction enthalpies were calculated; these compare well with known values. More extensive calculations on the BF_3/BF_4^- system indicate the structures and enthalpies are nearly converged with respect to basis set size and level of correlation treatment. The previously unknown species $B_2Cl_7^-$ is predicted to be energetically stable on the basis of the

* Author to whom all correspondence should be addressed.

Journal of Computational Chemistry, Vol. 17, No. 15, 1696–1711 (1996)

CCC 0192-8651 / 96 / 151696-16

calculations. Some features of the ^{11}B NMR spectra of room temperature melts consisting of mixtures of boron trichloride with 1-methyl-3-ethylimidazolium chloride are presented. These features suggest that these melts may contain small amounts of $B_2Cl_7^-$ as an intermediate in an exchange reaction.

Introduction

The common halides of aluminum and boron form an interesting class of compounds. Many of the neutral members are powerful Lewis acids and are frequently used as catalysts in synthetic chemistry, principally for Friedel–Crafts reactions.[1] Molten mixtures of aluminum halide salts are of technological importance for their use in the production of aluminum metal. Related melts may see application as electrolytes for high energy density batteries; when used as solvents these melts are also known to support novel redox and coordination chemistry.[2] The electronic and geometric structures of many of the components of these melts have been studied with semiempirical,[3] density functional theory (DFT),[4] and *ab initio*[5] methods.

We have approached this study with the goal of interpreting some results in molten salt chemistry. Bock et al.[5f] have show that it is possible to compute with *ab initio* molecular orbital (MO) methods results that are in very good agreement with spectroscopic measurements of molten salts, even at rather high temperatures.[6] Most molten salt systems have high liquidus temperatures. The number of ionic systems that are liquid at room temperature or below is rather limited and includes those reviewed by Hussey[7] and a few others.[8–10] We reported a tetrachloroborate melt that is liquid at and somewhat below room temperature.[11] In that work we characterized the melt via Raman spectroscopy and electrochemical methods. We expected to detect $B_2Cl_7^-$ in this system under acidic conditions, because the related species $Al_2Cl_7^-$ (refs. 12, 13) and $Ga_2Cl_7^-$ (ref. 9) are well known in similar melts, and $B_2F_7^-$ has been detected using ^{19}F NMR.[14] Despite this expectation there were no Raman bands of the chloroborate melts that could be attributed to $B_2Cl_7^-$.

The use of NMR methods for boron compounds has been well documented.[15] NMR measurements of boron containing neutral and ionic species expected in this melt system (BCl_3, BCl_4^-) have been reported.[16,17] These NMR studies have included solids[18] and aqueous as well as nonaqueous solutions.[19,20]

Experimental

COMPUTATIONS

All of the calculations were performed using Gaussian 92 or Gaussian 94[21] on a CRAY-YMP computer. Initial geometries for each species were based on known structures, either for that species or for a related species. Species known to possess symmetry (principally T_d for $AlCl_4^-$ and related species, D_{2h} for Al_2Cl_6 and related species, and D_{3h} for $AlCl_3$ and related species) were optimized within that symmetry. Initial calculations were carried out on $Al_2Cl_7^-$. For this species geometry optimizations were carried out for each of seven possible symmetries at the restricted Hartree–Fock (RHF) level with the following basis sets: STO-3G, 3-21G, 6-31G, 6-G(*d*), 6-31 + G, 6-31 + G(*d*), and 6-311 + G(*d*). Because these showed that the lowest energy occurred for C_1 symmetry, this point group was used for species related to $Al_2Cl_7^-$. For each species, vibrational frequencies for the RHF/6-311 + G(*d*) geometry were calculated at the RHF/6-311 + G(*d*) level; energies for each were also calculated at the MP2/6-311 + G(*d*) level. For some of the smaller species geometries were optimized at the MP2/6-311 + G(*d*) level. The effects of larger basis sets and more sophisticated treatment of electron correlation were investigated for the smallest species: BF_3, BF_4^-, and F^-. Single point energies for these were calculated at the MP2, MP4, and QCISD(*t*) levels, with the 6-311 + G(*d*) basis set, and geometries for BF_4^- were optimized at the MP2/6-311 + G(*d*), MP2/6-311 + G(*df*), MP2/6-311G(2*df*), MP2/ 6-311 + G(3*df*), and QCISD/6-311 + G(*d*) levels. All MP2 (and other correlated) calculations were done using frozen core orbitals. All of the final results (for anions and neutrals) were computed with the inclusion of diffuse functions (indicated by the +

sign) in the basis set for each atom. The Gauge-Independent Atomic Orbital (GIAO) method in Gaussian 94 were used to compute ^{11}B NMR chemical shifts for the boron containing species in the melt samples at the RHF/6–311 + G(*d*) level, using geometries optimized at that level.

NMR

Melt samples were prepared in medium wall thickness, 10-mm diameter NMR tubes. The tubes were weighed and introduced into an inert atmosphere dry box where a weighed amount of purified 1-methyl-3-ethylimidazolium chloride[11] (MEIC) was introduced into each tube. The tubes were transferred to a vacuum line, chilled to 77 K, and then a known volume of BCl_3 was distilled into each tube. The tubes were flame sealed and allowed to warm to room temperature. Both the sealed and open parts of each tube were weighed again. The compositions of the mixtures prepared in this manner are known up to better than 1%. NMR spectra were measured with a JEOL FX90Q spectrometer equipped with a variable temperature sample probe. The ^{11}B resonance of BF_3 etherate was used as an external standard. In the variable temperature studies spectra were obtained successively starting with ambient temperature and cooling to the lowest temperature obtainable (without freezing the melt). The following procedure was used: the cooled sample was allowed to equilibrate for 15 min, a spectrum was then obtained followed by an additional 15-min equilibration and another spectral measurement. There was no difference between the two spectra for any of the temperatures studied; this implies that thermal and mechanical equilibrium had been reached during the first 15 min. Finally, 200 spectra were averaged; the spectrum was plotted using a normal and a 50-fold ordinate expansion.

Results

CALCULATIONS

The energies at the MP2/6–311 + G(*d*)//RHF/6–311 + G(*d*) level, and the zero point vibrational energies [RHF/6–311 + G(*d*)//RHF/6–311 + G(*d*)] for each species studied are presented in Table I. The structures of most of the species are presented in Figure 1. The results of geometry optimizations are presented in Table II.

TABLE I.
Electronic and Vibrational Energies.

Species	Energy (au)[a]	ZPE (kJ/mol)[b]
$AlCl_3$	−1 621.130 10	13.20
	(−1 621.130 14)	
$AlCl_4^-$	−2 080.960 29	16.03
	(−2 080.960 56)	
Al_2Cl_6	−3 242.311 93	30.08
	(−3 242.312 78)	
$Al_2Cl_7^-$	−3 702.145 34	31.55
AlF_3	−541.239 55	21.15
AlF_4^-	−641.102 18	26.75
Al_2F_6	−1 082.557 55	48.97
$Al_2F_7^-$	−1 182.429 34	52.14
BCl_3	−1 403.840 38	20.97
BCl_4^-	−1 863.622 32	22.93
$B_2Cl_6^-$	−2 807.662 39	42.05
$B_2Cl_7^-$	−3 267.479 31	44.36
BF_3	−323.982 75	34.24
BF_4^-	−423.791 90	39.02
	(−423.793 07)	
B_2F_6	−647.947 66[c]	70.42[c]
	−647.969 57[d]	69.65[d]
$B_2F_7^-$	−747.809 86	75.72
F^-	−99.678 68	
Cl^-	−459.703 57	
Al_2Cl_5F; bridging fluorine	−2 882.364 00	33.74
Al_2Cl_5F; terminal fluroine	−2 882.349 03	32.94
$Al_2Cl_6F^-$; bridging fluorine	−3 342.208 98	35.39
$Al_2Cl_6F^-$; terminal fluorine	−3 342.182 21	34.32

[a] Energy is at the MP2/6–311 + G(*d*)//RHF/6–311 + G(*d*) level; for some species the MP2/6–311 + G(*d*)//MP2/6–311 + G(*d*) level energy is given in parentheses.

[b] Zero point energies are from unscaled frequencies at the RHF/6–311 + G(*d*)//RHF/6–311 + G(*d*) level.

[c] Vibrational frequencies indicate that this species (D_{2h} symmetry) is a transition state; it has one large, imaginary vibrational frequency (235*i* cm^{-1}); the corresponding mode is a dissociation into monomers along a B_{2g} symmetry coordinate.

[d] This species has C_{2h} symmetry and has one small imaginary frequency (14*i* cm^{-1}); the corresponding mode is of B_u symmetry. The quoted "zero point energy" for these species is the total vibrational energy for the 17 real frequencies at 0 K.

The computed structures for MX_4^- agree very well with those computed previously.[3b,5g–i] The computed vibrational frequences (and experimental values where they are known) for each species are given in the Appendix.

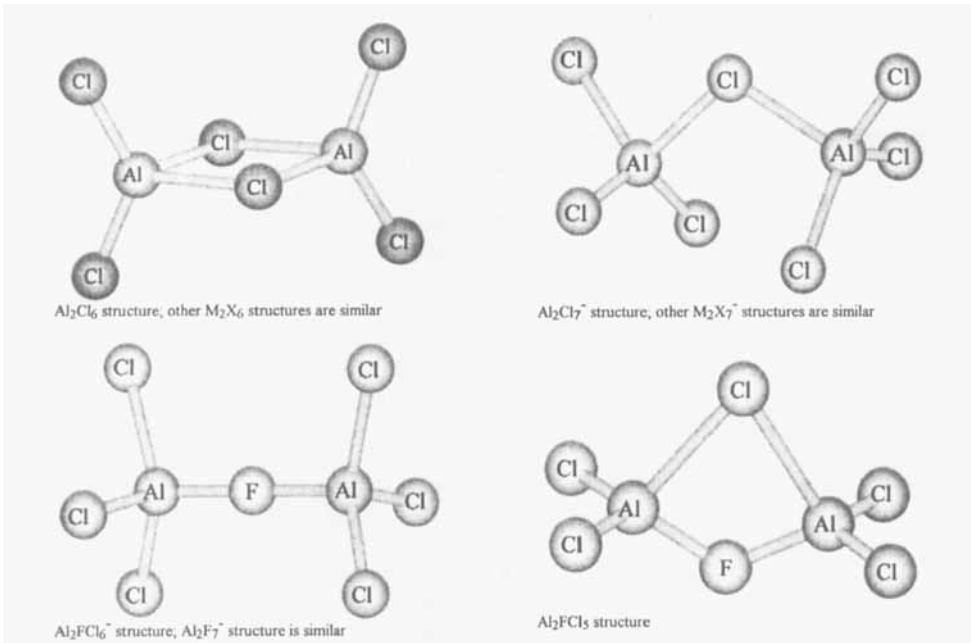

Al_2Cl_6 structure; other M_2X_6 structures are similar

$Al_2Cl_7^-$ structure, other $M_2X_7^-$ structures are similar

$Al_2FCl_6^-$ structure; $Al_2F_7^-$ structure is similar

Al_2FCl_5 structure

FIGURE 1. Geometries for the dimeric species under study here. Structural details are presented in Table II.

ALUMINUM HALIDES

Unlike the other aluminum halides in this study for which the geometry is well known, it is not clear what symmetry is appropriate for calculations on $Al_2Cl_7^-$. To investigate this, geometry optimizations were performed on seven different structures of this anion. These structures differ in orientation of the two $AlCl_3$ units relative to the central Al-Cl-Al bridge. There are two high symmetry structures, one with D_{3h} and one with D_{3d} symmetry. There are two structures with C_{2v} symmetry; these have a plane defined by a Cl-Al-Cl-Al-Cl linkage that is either W or C shaped, with the two $AlCl_3$ units related by a reflection plane. There is one C_s structure where the Cl-Al-Cl-Al-Cl plane is retained, but the mirror symmetry of the two $AlCl_3$ units is lost. There is one C_2 structure where the rotational symmetry is retained but the reflection planes are both lost. Finally there is a structure with no symmetry (the Cl-Al-Cl-Al-Cl atoms are no longer in the same plane). For most of these structures, full optimizations were performed at the RHF level with the following basis sets: STO-3G, 3-21G, 6-31G, 6-31 + G, 6-31G(d), 6-31 + G(d), and 6-311 + G(d). Optimizations at the RHF/6-311 + g(d) level were computed for each structure. For each basis set the structure with C_1 symmetry had the lowest energy, except that the structure with C_2 symmetry has the same energy (−3701.06785 au) at the RHF/6-311 + g(d) level as the C_1 structure. Vibrational frequency calculations at this level indicate that these structures are both minima; the vibrational zero point energy of the C_1 structure is about 0.004% lower than the C_1 structure. The average bond lengths and angles do not differ significantly for these two structures; the reported geometrical parameters are for the C_1 structure. Rather surprisingly, the bond lengths from the STO-3G calculation were in the best agreement with the known crystal structure for this anion,[22] with the 6-311 + G(d) calculations next best. Following the notation of Table II, the STO-3G structure was found to be: Al-Cl term.: 2.088, [2.102]; Al-Cl bridg.: 2.236, [2.242]; Cl-Al-Cl bridg.: 131.2 [110.8]. Despite the somewhat poorer agreement on bond lengths for this anion, the 6-311 + G(d) basis set was used for most of the rest of this study. We found that there was little improvement in the agreement between the calculated structure and the experimental one when the self-consistent reaction field (SCRF)[23] method was used during the optimization, with "solvent" dielectric constants ranging from 2 to 100. The 6-311 + G(d) basis set yields rather good structures for most of the other species in this study. It is interesting to note that for Al_2Cl_6 this basis set gives a very good structure at the RHF level, and a structure that is essentially in perfect agreement with the known structure[24] at the MP2 level. These results are in slightly better agreement with the

TABLE II.
Optimized Structures.

Species	Symmetry	Structure[a]	Reference
$AlCl_3$	D_{3h}	Al-Cl: 2.073, (2.067), [2.068]	40
$AlCl_4^-$	T_d	Al-Cl: 2.165, (2.149), [2.11-2.16]	37
Al_2Cl_6	D_{2h}	Al-Cl term.: 2.079, (2.071), [2.07] Al-Cl bridg.: 2.282, (2.258), [2.25] Cl-Al-Cl term.: 121.9, (123.3), [123.4] Cl-Al-Cl bridg.: 89.3 (91.3), [91]	24
$Al_2Cl_7^-$	C_1	Al-Cl term.: 2.126, [2.102] Al-Cl bridg.: 2.313, [2.242] Cl-Al-Cl bridg.: 123.1 [110.8]	22[b]
AlF_3	D_{3h}	Al-F: 1.631, [1.631]	41a
AlF_4^-	T_d	Al-F: 1.692, [1.69]	41b
Al_2F_6	D_{2h}	Al-F term.: 1.631, (1.654) Al-F bridg.: 1.803, (1.826) F-Al-F term.: 124.0, (125.4) F-Al-F bridg.: 78.7, (79.8)	
$Al_2F_7^-$	D_{3d}	Al-F term.: 1.667, (1.690) Al-F bridg.: 1.780, (1.799)	
BCl_3	D_{3h}	B-Cl: 1.748, (1.739), [1.75]	42
BCl_4^-	T_d	B-Cl: 1.876, [1.84]	43
B_2Cl_6	D_{2h}	B-Cl term.: 1.776 B-Cl bridg.: 1.993 Cl-B-Cl term.: 118.5 Cl-B-Cl bridg.: 92.0	
$B_2Cl_7^-$	C_1	B-Cl term.: 1.826 B-Cl bridg.: 2.080 Cl-B-Cl bridg.: 120.2[b]	
BF_3	D_{3h}	B-F: 1.298, [1.31]	42
BF_4^-	T_d	B-F: 1.395, [1.43]	37
B_2F_6	D_{2h}	B-F term.: 1.300 B-F bridg.: 1.536 F-B-F term.: 122.6 F-B-F bridg.: 85.7	
B_2F_6	C_{2h}	B-F term.: 1.296 B-F bridg.: 1.305; 3.001 F-B-F term.:120 F-B-F bridg.: 70.7	
$B_2F_7^-$	C_1	B-F term.: 1.353 B-F bridg.: 1.565 F-B-F bridg.: 139.1[b]	
Al_2Cl_5F; bridging F	C_{2v}	Al-F bridg.: 1.806 Al-Cl bridg: 2.291 Al-Cl term.: 2.074 Al-F-Al: 112.7 Al-Cl-Al: 82.0 Cl-Al-Cl term.: 123.2	
Al_2Cl_5F; terminal F	C_s	Al-Cl bridg: 2.394 Al-F term.: 1.673 Al-Cl term.: 2.16 Cl-Al-Cl bridg.: 84.3 Al-Cl-Al: 95.6 Cl-Al-X term.: 123.6[c]	
$Al_2Cl_6F^-$; bridging F	D_{3d}	Al-Cl term.: 2.128, (2.115) Al-F bridg.: 1.792, (1.802)	
$Al_2Cl_6F^-$; terminal F	C_1	Al-Cl term.: 2.126 Al-F term.: 1.662 Al-Cl bridg.: 2.308 Al-Cl-Al: 122.2[b]	

[a] Structural parameters are from optimizations at the RHF/6-311 + $G(d)$ level for all species; for some species results from MP2/6-311 + $G(d)$ optimizations are given in parentheses. Experimental values are given in brackets. Bond lengths are given in Ångstroms and angles in degrees.
[b] Bond lengths are the averages of the two bridging bond lengths and the average of the six (or five) terminal bond lengths.
[c] The four bridge bond lengths are averaged, as are the three Al-Cl terminal bond lengths and the terminal bond angles.

experimental structure than the recent RHF/6-31$G(d)$ calculations by Bock et al.[5e]

For Al_2F_6 there is no known experimental structure. The electron diffraction methods used for the other aluminum halide dimers[24] may be too difficult for the fluoride because its low volatility requires much higher temperatures, and at these high temperatures only a very small fraction of the vapor is in the dimer form.[25] Our calculations with the 6-311 + $G(d)$ basis set gives slightly longer

bond lengths for this species at both the RHF and MP2 levels than the recent calculations of Bock et al.[5e] with the 6–31G(*d*) basis set. Initial attempts to optimize the geometry for $Al_2F_7^-$ in the C_1 symmetry appropriate for $Al_2Cl_7^-$ failed, as the Al-F-Al bond angle approached linearity. The structure had almost perfect D_{3d} symmetry. Computation of vibrational frequencies for the RHF/6–311 + *G*(*d*) structure in D_{3d} symmetry showed it to be an energy minimum. Gilbert et al.[6] suggested that the small size of a fluorine atom might make the Al-F-Al linkage linear. Because it is likely that the halogens in $Al_2F_7^-$ are more highly charged than in $Al_2Cl_7^-$, a linear Al-F-Al linkage will maximize the separations between the halogens, thus minimizing electrostatic repulsion. Our results are consistent with this suggestion by Gilbert and colleagues, and with the somewhat lower level calculations of Curtiss.[5m]

Gilbert et al.[6] used Raman spectroscopy to study the properties of chloroaluminate melts containing fluoride. These melts contain a variety of fluorine substituted aluminum chloride species. The monomeric species have been well studied at the HF and MP2 level by Bock et al.[5f] There are four possible species that can be formed with a single fluorine substitution in the aluminum chloride dimer. The computed structures for these are presented in Table II. It is interesting to note that the F bridged $Al_2Cl_6F^-$ has the same D_{3d} symmetry as $Al_2F_7^-$.

BORON HALIDES

Many of the features for the aluminum halides are reproduced in the corresponding boron species. There are, however, some significant differences. Unlike the aluminum species, the neutral boron halides are not known to form dimers at room temperature. Our results are consistent with this, in that computations of the vibrational frequencies for B_2F_6, show this species to be a transition state. Also, as will be described in more detail below, B_2Cl_6 is not a transition structure, but is higher in energy than two isolated monomers. It is known that mixtures of boron halide monomers undergo rapid halogen exchange[26]; our results strongly suggest that a D_{2h} type dimer structure is involved as an intermediate in these exchange processes.

There are subtle, but significant differences in the isotopic intensities in the gas and condensed phases seen in the Raman spectrum of BCl_3. Loewenschuss[27] has shown that these are due to intermolecular association between the monomer molecules in the condensed but not the gas phase. Edwards et al.[28] suggested that this association takes the form of a B_2Cl_6 molecule with a single chlorine bridge. We attempted to find such a structure of this type, but all of our attempts (at the RHF level with small to quite large basis sets) failed: the structure appears to dissociate. These authors also suggest that in the liquid phase, the formation of B_2Cl_6 from monomers is very slightly exothermic; this is not consistent with our computations for gas phase species.

B_2F_6 is not known in the gas phase, but it has been observed in low temperature inert gas matrix isolation studies.[29] In these studies it was assumed that the molecule had the D_{2h} structure of Al_2Cl_6, but Nxumalo and Ford[5j] recently used RHF/6–31(*d*) calculations to suggest that a C_{2h} structure is a better description for this species. Our calculations do show this structure (two nearly planar, parallel BF_3 units connected by two weak, long B—F bonds in a plane orthogonal to the BF_3 units) to have a lower energy; but even after optimization with the tight and calcall options at the RHF/6–311 + (*d*) level, it still has a single negative Hessian eigenvalue. At this level both structures are transition states. Results for both of these structures are presented below.

NMR chemical shifts were computed at the RHF/6–311 + (*d*) level for B in BCl_3, BCl_4^-, $B_2Cl_7^-$, and $BF_3 \cdot O(C_2H_5)_2$. The isotropic part of the magnetic shielding tensor was found to be 66.7, 106.7, 100.6, and 120.3 ppm, respectively. The last species is the standard for B NMR; these results suggest that the ^{11}B resonance for these species should be observed at 53.6, 13.6, and 19.7 ppm.

As will be shown below, our conclusions in this study depend to some degree on computed reaction enthalpies. Some of these may be compared to experimental values; but no experimental data exist for many reactions involving these species, particularly those involving anions. Hence our confidence in these enthalpies must rely on more sophisticated theoretical calculations. The boron fluoride system provides a convenient choice for this comparison, because it is typical of many of these reactions. Its relatively small size allows calculations with much larger basis sets or more sophisticated treatment of electron correlation. Table III presents the electronic energies for F^-, BF_3, and BF_4^- calculated at the RHF/6–311 + *G*(*d*) geometry, with correlated methods from MP2/6–311 + *G*(*d*) through QCISD(*t*)/6–311 + *G*(*d*), and with basis sets as large as 6–311 + *G*(3*df*). The

TABLE III.
Effects of Correlation and Basis Set on Boron Fluoride Energies.

Method \ Species	F^-	BF_3	BF_4^-
RHF/6-311 + G(*d*)	−99.445 65	−323.284 80	−422.862 27
MP2/6-311 + G(*d*)	−99.678 68	−323.982 75	−423.791 90
MP3/6-311 + G(*d*)	−99.666 89	−323.971 14	−423.775 20
MP4*D*/6-311 + G(*d*)	−99.671 97	−323.981 22	−423.788 71
MP4*DQ*/6-311 + G(*d*)	−99.671 73	−323.976 22	−423.782 33
MP4*SDQ*/6-311 + G(*d*)	−99.676 43	−323.984 89	−423.793 49
MP4*SDTQ*/6-311 + G(*d*)	−99.684 42	−324.004 91	−423.819 53
QCISD/6-311 + G(*d*)	−99.675 91	−323.985 25	−423.793 84
QCISD(*T*)/6-311 + G(*d*)	−99.680 60	−324.001 03	−423.814 48
MP2/6-311 + G(*df*)	−99.700 03	−324.087 82	−423.923 52
MP2/6-311 + G(2*df*)	−99.724 81	−324.146 98	−424.004 02
MP2/6-311 + G(3*df*)	−99.732 13	−324.161 09	−424.023 72

Energies are calculated at the RHF/6-311 + G(*d*) geometry, and are given in atomic units. All of the correlation energies are calculated with frozen core orbitals.

results presented in Table II show that in general, the structures computed in this study that are in closest agreement with the experiment are the neutral molecules, whose experimental structures are generally determined by gas phase electron diffraction. The agreement is slightly poorer for the anions. This is due at least in part, to the fact that the experimental structures are all from condensed phase measurements, while the calculations yield what are best regarded as dilute gas phase structures. BF_4^- also provides a convenient species to compare anion structures at various levels of theory. The structure of BF_4^- was computed with a variety of basis sets; the B—F bond lengths that were found are presented in Table IV.

NMR SPECTROSCOPY

The compositions of the melts reported in this study range from slightly acidic (mole fraction of BCl_3 greater than 0.5) to pure BCl_3. Mole ratios of BCl_3:MEIC of 100:0, 83:17, 58:42, and 52:48 were used. It was not possible to study the NMR spectra of basic melts because of limited solubility of MEIC in basic melts at room temperature.[11] The pure BCl_3 and the 52:48 samples are homogeneous liquids while in the other two samples two phases were present, melt and pure BCl_3.[11] The spectra reported for the 58:42 sample were measured with only the melt phase present in the active volume of the NMR tube. The 83:17 sample had both liquid phases present in the active volume of the tube.

TABLE IV.
Effects of Correlation and Basis Set on BF_4^- Structure.

Method	B-F Bond Length (Å)
RHF/6-311 + G(*d*)	1.395
MP2/6-311 + G(*d*)	1.415
MP2/6-311 + G(*df*)	1.404
MP2/6-311 + G(2df)	1.406
MP2/6-311 + G(3df)	1.406
QCISD/6-311 + G(*d*)	1.412

Optimizations were constrained to T_d symmetry; all correlated methods used frozen core orbitals.

The NMR spectra for these samples are simple (Fig. 2): for a single phase a single peak is observed while for two phases two peaks are seen. Thus, the spectra consist of either a single narrow peak near 46 ppm, or a single, somewhat broader peak near 13 ppm, or both. As the melt becomes more acidic, the peak near 13 ppm shifts slightly downfield, and its width increases. The peak near 46 ppm (present only in the spectra of pure BCl_3 and the 83:17 sample) does not exhibit significant changes with melt composition.

The NMR spectra of these samples were measured as functions of temperature between room temperature and just above the freezing points for the melts (about −12°C for the most acidic melts).[11] The results of these measurements are summarized in Table V. The position of the highest field peak shifts from about 10 to 13 ppm as the melt becomes more acidic, and its width at room temperature increases from about 13 Hz for the least acidic to about 26 Hz for the most acidic. For

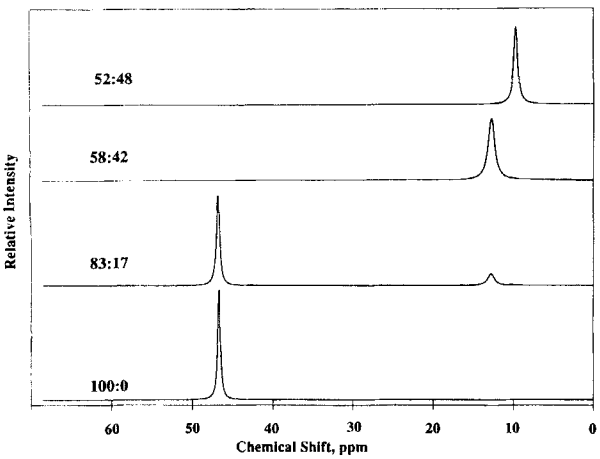

FIGURE 2. ^{11}B NMR spectra of BCl_3:MEIC liquid mixtures at room temperature. Liquid compositions are given as mole percent of BCl_3:MEIC. Chemical shifts are relative to a BF_3:etherate external standard.

each composition the peak position does not change significantly over the temperature range studied, but the width of this peak increases dramatically from 13 Hz for the least acidic melt at room temperature to 107 Hz for the most acidic melt at $-10°$ C.

An interesting phenomenon was observed with the 58:42 sample: when the NMR tube was removed from the probe after measurement at 0 and $-10°$ C, the melt had a cloudy appearance. This cloudiness disappeared when the sample was warmed to room temperature. In addition, the spectra for this sample at reduced temperatures showed a very small peak near 46 ppm; the intensity of this peak increased relative to that of the much larger peak near 13 ppm as the temperature was lowered. A 50-fold ordinate expansion was used together with a cut and weigh integration method to find the relative integrated intensities of these two peaks. The results of this integration are presented in Table VI.

TABLE VI.
Relative Areas for Peaks for 58:42 Melt at Various Temperatures.

Temperature (° C)	Area 13-ppm Peak	46-ppm Peak
24.2	100.0	0.0
15.1	99.86	0.136
5.1	99.66	0.324
−4.7	99.53	0.467
−10.2	99.42	0.579

Relative areas have an uncertainty of ±10%.

Discussion

NMR SPECTROSCOPY

The following information may be deduced from the NMR data presented above: the identity of the major boron containing species in these samples (these may include BCl_3 and BCl_4^-); the solubility of BCl_3 in the acidic melt; and the existence of minor boron containing species, especially $B_2Cl_7^-$.

Major Species

Inspection of Table I and Figure 2 makes it clear that the peak near 46 ppm in the spectrum of the 83:17 melt sample is due to BCl_3. This is expected for this sample because both the melt phase and pure BCl_3 are present in the measured volume of the sample tube. The other peak in the spectrum of this sample at about 13 ppm must be due to BCl_4^-.

TABLE V.
Variation in Position and Width of NMR Peaks with Composition and Temperature.

	Temperature							
	25°C		10°C		0°C		−10°C	
Composition	Position	Width	Position	Width	Position	Width	Position	Width
52:48	9.7	13.4	9.6	26.9	9.6	39.1	Frozen	
58:42	13.1	26.9	12.7	40.3	12.7	59.8	12.8	101.3
83:17	13.1	25.6	12.6	42.0	12.8	57.4	12.6	107.5
	47.0	15.9	46.5	19.0	46.7	15.8	46.7	23.2
100:0	46.6	12.2	46.7	12.2	46.6	12.2		

Positions are given in parts per million (ppm) from the BF_3:etherate external reference and have an uncertainty of ±0.5 ppm. Widths are full width at half maximum and are given in Hertz; they have an uncertainty of ±0.5 Hz.

These assignments are in fair agreement with the chemical shifts computed for these species.

These assignments are consistent with the work of Phillips et al.[16] who reported a shift of 47.4 ppm for BCl_3, and with Landesman and Williams[17] who reported the BCl_3 shift at 45.6 ppm and BCl_4^- shift at 11–12 ppm. They are also consistent with Hartmen and Schrobilgen[30] who reported the BCl_4^- shift at 11.6 ppm in methylene chloride. The assignment of the peak near 13 ppm in our spectra to BCl_4^- is not consistent with the work of Thompson and Davis[31] who report a shift of 6.6 ppm for BCl_4^- in dimethylsulfoxide and HCl. This latter inconsistency is not surprising because it is known that the chemical shift of this anion moves upfield with increasing chloride concentration in the solvent.[17] Because the samples studied here range from slightly to strongly acidic, the chloride concentration should be very low because chloride is a base. The solvent used by Thompson and Davis[31] was quite rich in chloride. Indeed, the chemical shifts that we observe for BCl_4^- in the strongly acidic (two phase) melts (about 13 ppm) indicate that the free Cl^- concentration in these samples must be very low.

These considerations of chemical shifts confirm the previous Raman spectroscopic results that the major boron containing species in these melts in BCl_4^-. It should be noted that even though the strongly acidic melts are approximately 1 molar in BCl_3, as shown with Raman spectroscopy,[11] no peak in the NMR spectrum of the 58:42 melt that can be attributed to BCl_3 is observed.

Solubility Equilibrium

The solubility of BCl_3 in these tetrachloroborate melts is limited. The equilibrium may be expressed as follows:

$$BCl_{3(\text{pure liquid})} \Leftrightarrow BCl_{3(\text{solution})}.$$

Raman spectroscopy was used to show that in the saturated (two phase) melt BCl_3 is present.[11] The concentration of BCl_3 in the melt can be found from the Raman spectra by using the areas of the ν_1 Raman band of BCl_3 in the saturated melt and in the pure liquid, and the density of BCl_3 at 25°C [1.33 g/cm^3 obtained by linear extrapolation of the density values at −78° C of 1.48 g/cm^3 (measured) and 0° C of 1.37 g/cm^3 (taken from ref. 32)]. These gave a concentration of BCl_3 in the saturated melt at 25° C of 0.86 ± 0.04 M, corresponding to a BCl_3 mole fraction of 0.17 ± 0.01.

The thermodynamics of the solubility equilibrium of BCl_3 in the acidic melt were investigated by varying the temperature of the melt and measuring the changes in the spectra. The results of these measurements are summarized in Table VI. The interpretation of the data in Table VI is simple: as the temperature of the melt is lowered, the solubility of BCl_3 is decreased, and some of the BCl_3 precipitates as tiny droplets. Because the density of the BCl_3 differs from that of the melt by only about 7%, and the melt is rather viscous, the resulting emulsion is stable during the time required for the NMR experiment. The relative areas of the "BCl_4^-" peak at 13 ppm compared to the BCl_3 peak at 46 ppm were used to measure the temperature dependence of the solubility of BCl_3. The rationale for this procedure is as follows: the spectrum of the 58:42 melt at room temperature has a single peak at 13 ppm (BCl_4^- chemical shift), even though the sample is about 0.9 M in BCl_3. Thus the intensity of the peak at 13 ppm must be due to a coalescence of the BCl_4^- and BCl_3 resonances, implying that these species must be in equilibrium. Because the mole fraction of BCl_3 is quite low, this coalescence (13 ppm) results in a peak much closer to the BCl_4^- resonance (9.7 ppm) than to the BCl_3 resonance (46.6 ppm). Hence when the temperature is lowered and BCl_3 comes out of solution, the intensity of the small BCl_3 peak must come at the expense of the contribution that BCl_3 in solution makes to the intensity of the peak at 13 ppm.

Figure 3 is a Van't Hoff plot of the temperature dependence of the solubility of BCl_3 in the melt.

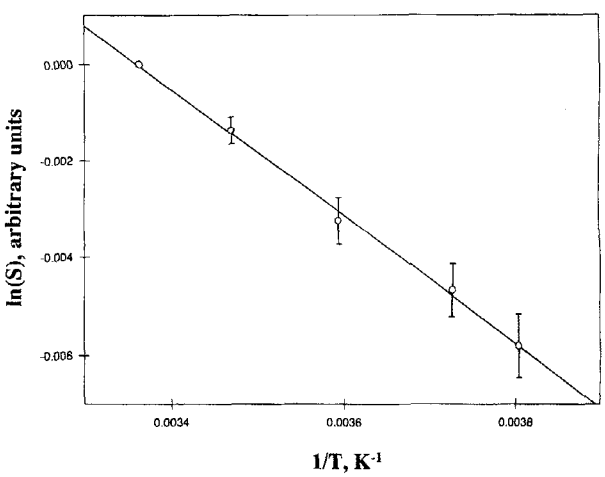

FIGURE 3. Van't Hoff plot of the solubility of BCl_3 in the acidic BCl_3:MEIC melt as a function of temperature. The error bars indicate the absolute errors in the NMR peak integration.

The slope of this plot gives 110 ± 30 J/mol for the integral heat of solution of BCl_3 in the melt. Using the mole fraction of BCl_3 in solution at room temperature and assuming unit activity coefficients, the Gibbs free energy of solution is found to be 4.6 ± 0.3 kJ/mol (using $\Delta G = -RT \ln K_x$), and the entropy of solution is -14 ± 4 J/molK. Because one would expect a solution to be less ordered than two pure liquids, this negative value for the solution entropy is quite unexpected and begs an explanation. The negative value for the entropy of solution together with the absence of a BCl_3 peak in the spectrum, strongly suggests that the solution is more complex than a simple molecular solution of BCl_3.

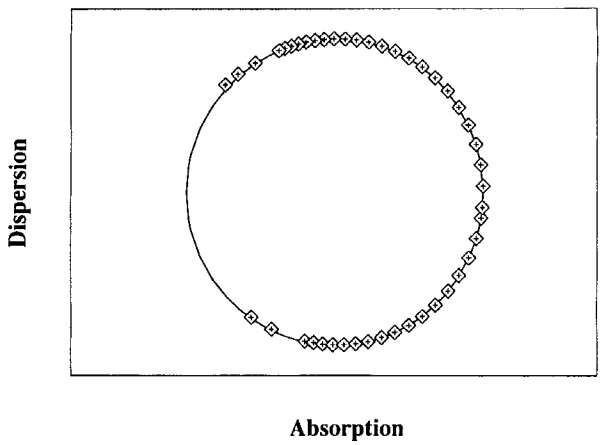

FIGURE 4. DISPA plot for the 58:42 NMR spectrum from Figure 2.

Minor Species

Raman spectroscopy shows that a saturated solution of BCl_3 in the melt is about 0.9 *M* in BCl_3.[11] This is more than enough BCl_3 to give a well-defined signal in the NMR spectrum of a melt saturated with BCl_3, yet no signal that can be attributed to BCl_3 in solution is observed. This implies that an exchange equilibrium is present in the solution, and that the rate of this exchange is faster than the NMR time scale, but slower than the Raman time scale:

$$B^*Cl_4^- + BCl_3 \Leftrightarrow BCl_4^- + B^*Cl_3.$$

This type of equilibrium, if its rate is sufficiently fast, will cause the BCl_3 and BCl_4^- resonances to coalesce, as is observed. Under equilibrium conditions when exchange rates are not too fast, DISPA (Dispersion Absorbance) analysis of the NMR spectrum will reveal the presence of the equilibrium and will do so with greater sensitivity than is possible by considering only the NMR linewidth. This method is a sensitive technique for investigating line broadening in magnetic resonance spectroscopies. In the DISPA method, both the absorption and the dispersion spectra are measured and normalized; the normalized dispersion is then plotted against the normalized absorption.[33] For a single Lorentzian peak this plot will be a perfect circle of unit radius, centered at (1/2, 0). Distortions from circularity give information about NMR dynamics in the sample. Figure 4 is a DISPA plot for the NMR spectrum of the 58:42 melt obtained at room temperature; the experimental points lie almost perfectly on the reference circle. The high degree of circularity for this plot indicates that on the time scale of the NMR measurement, the BCl_3 and BCl_4^- that contribute to the NMR peak are effectively a single chemical species. That is, the exchange rate for the above equilibrium is much faster than can be resolved on the NMR time scale. The clear presence of the ν_1 band of BCl_3 in the Raman spectra of these melts indicates that the exchange rate is quite slow on the Raman time scale.

There are two possible mechanisms through which the above exchange equilibrium could be achieved. The first is a chloride exchange:

$$\begin{aligned} B^*Cl_4^- &\Leftrightarrow B^*Cl_3 + Cl^-, \\ BCl_3 + Cl^- &\Leftrightarrow BCl_4^-, \end{aligned} \qquad (1)$$

and the second involves an intermediate,

$$\begin{aligned} B^*Cl_4^- + BCl_3 &\Leftrightarrow B^*Cl_4BCl_3^-, \\ B^*Cl_4BCl_3^- &\Leftrightarrow B^*Cl_3 + BCl_4^-. \end{aligned} \qquad (2)$$

The samples of interest here are all acidic, and the 83:17 and 58:42 samples are strongly acidic, as they are saturated with BCl_3. Because chloride ion is a base it is unlikely that the chloride activity in these melts is sufficiently large for mechanism (1) to apply. As discussed above, the chemical shift for BCl_4^- in the BCl_3 saturated samples is consistent with a very low chloride activity. In reactions between organotin chlorides and BCl_3, abstraction of chloride is not common,[34] which implies that this system also has a low Cl^- activity. These considerations (BCl_4^- chemical shift in the melt and low Cl^- activity in related systems) imply that free chloride is unlikely to be present in the chloroborate melt system.

Hence the second mechanism is more likely. The intermediate in this mechanism is $B_2Cl_7^-$, a species that has not been observed to the best of our knowledge. The valence isoelectronic heptafluorodiborate anion was investigated using ^{19}F NMR spectroscopy.[14] In this work the sample had to be cooled below $-100°$ C before the resonance of $B_2F_7^-$ could be resolved into terminal and bridging F signals, and below $-150°$ C before the splitting of the terminal F signal could be resolved. The expected splitting of the bridging F was not observed before the sample froze. If $B_2Cl_7^-$ exists in our melt samples it would be expected to exhibit similar exchange and cannot be resolved because the melts solidify at about $-12°$ C.[11] The GIAO calculations suggest that if $B_2Cl_7^-$ had a sufficiently long lifetime its ^{11}B resonance would be near 20 ppm where it would not overlap any of the peaks in Figure 2.

To investigate the likelihood of the existence of the $B_2Cl_7^-$ anion, we used *ab initio* MO calculations to investigate the proposed $B_2Cl_7^-$ as well as many closely related species such as the isoelectronic $B_2F_7^-$ and $Al_2Cl_7^-$.

MO CALCULATIONS

Energetics

The arguments presented below regarding $B_2Cl_7^-$ depend to some extent on the degree to which calculations of relative energies of these species may be trusted. In some cases experimental values of these relative energies are available in the form of reaction enthalpies; these values should be well reproduced by the calculations. In other cases experimental data is not available. For these cases comparisons with calculations at a higher level of theory may be made. Such data for comparison purposes is presented in Table VII; these are values for ΔH_{0K} for the formation of tetrafluoroborate. The layout follows that of Table III. The reaction enthalpies are calculated from the data in Tables I and III using standard methods.[35] In each case in this table the energy for each species was calculated with the indicated method, using the RHF/6–311 + $g(d)$ geometry. Corrections for the vibrational zero point energies were made using unscaled frequencies calculated at the RHF/6–311 + $g(d)$ level.

The reaction enthalpy calculated at the MP2 level with the very large 6–311 + $g(3df)$ basis set is quite close to that calculated with the more modest 6–311 + $g(d)$ basis set. This suggests that the MP2 energies are nearly converged with respect to basis set size when the more modest 6–311 + $g(d)$ basis set is used. The reaction enthalpy calculated at the MP2/6–311 + $g(d)$ level differs only slightly from the values computed with the more accurate (and much more expensive) MP4SDTQ and QCISD(T) methods with this basis set. At worst the difference is only about 6 kJ/mol, an amount that is probably less than the uncertainty in most experimental reaction enthalpies. The data in Table VII support use of MP2/6–311 + $g(d)$ energies with RHF/6–311 + $g(d)$ vibrational corrections for investigation of reaction enthalpies involving the species covered in this article. The method appears to do a reasonable job of accounting for basis set size effects as well as electron correlation effects. It is known that the use of diffuse functions in the basis set is important for the accurate calculation of reaction enthalpies in the closely related Be-F system[36]; they are used in this method.

Table VIII lists reaction enthalpies for other formation reactions. These were all computed from MP2/6–311 + $g(d)$//RHF/6–311 + $g(d)$ energies as described above. For the two cases where experimental enthalpies are available (Al_2Cl_6 and Al_2F_6),[1,25] the vibrational frequencies were used to calculate the enthalpy at the temper-

TABLE VII.
Effects of Correlation and Basis Set on Reaction Enthalpies.

Method	ΔH_{0K} for $BF_3 + F^- \Rightarrow BF_4^-$ (kJ/mol)
RHF/6–311 + $G(d)$	−340.73
MP2/6–311 + $G(d)$	−337.17
MP3/6–311 + $G(d)$	−354.73
MP4D/6–311 + $G(d)$	−350.40
MP4DQ/6–311 + $G(d)$	−347.42
MP4SDQ/6–311 + $G(d)$	−341.64
MP4$SDTQ$/6–311 + $G(d)$	−336.48
QCISD/6–311 + $G(d)$	−342.97
QCISD(T)/6–311 + $G(d)$	−343.42
MP2/6–311 + $G(df)$	−350.83
MP2/6–311 + $G(2df)$	−341.77
MP2/6–311 + $G(3df)$	−337.26

Energies are calculated at the RHF/6–311 + $G(d)$ geometry. All of the correlation energies are calculated with frozen core orbitals.

TABLE VIII.
Computed Gas Phase Reaction Enthalpies.

Reaction	$\Delta H_{0\,K}$ (kJ/mol)	Product Known to be Stable?[a]
$2\,AlCl_3 \Rightarrow Al_2Cl_6$	−131.90[b]	Yes
$2\,AlF_3 \Rightarrow Al_2F_6$	−198.97[c]	Yes
$2\,BCl_3 \Rightarrow B_2Cl_6$	48.26	No
$2\,BF_3 \Rightarrow B_2F_6$	48.68[d]	No
	−9.50[e]	
$AlCl_3 + AlCl_4^- \Rightarrow Al_2Cl_7^-$	−141.71	Yes
$AlF_3 + AlF_4^- \Rightarrow Al_2F_7^-$	−225.39	Yes[g]
$BCl_3 + BCl_4^- \Rightarrow B_2Cl_7^-$	−43.06	?
$BF_3 + BF_4^- \Rightarrow B_2F_7^-$	−89.83	Yes
$Al_2Cl_6 + F^- \Rightarrow Al_2Cl_6F^-$ bridging F	−567.09[f]	?
$Al_2Cl_6 + F^- \Rightarrow Al_2Cl_6F^-$ terminal F	−497.98[f]	Yes
$Al_2Cl_6 + F^- \Rightarrow Al_2Cl_5F + Cl^-$ bridging F	−198.05[f]	?
$Al_2Cl_6 + F^- \Rightarrow Al_2Cl_5F + Cl^-$ terminal F	−159.62[f]	?

Enthalpies are calculated at the MP2/6−311 + $G(d)$//RHF/6−311 = $g(d)$ level with vibrational zero point energies from unscaled frequencies at the RHF/6−311 + $G(d)$//RHF/6−311 + $g(d)$ level. All of the correlation energies are calculated with frozen core orbitals.

[a] Yes indicates that the product is known in the gas phase at room temperature; No indicates that the product is known not to exist under these conditions; ? indicates that neither Yes nor No applies.

[b] The computed room temperature values for this is −127.4 kJ/mol; the experimental value at this temperature is −124.3 kJ/mol.[1]

[c] The computed value for this at 1000 K is −189.41 kJ/mol; the experimental value at this temperature is −200 ± 17 kJ/mol.[25]

[d] Frequency calculations show that this product is a transition structure; it has one large ($235i$ cm^{-1}) imaginary frequency. The corresponding normal mode is a dissociation into monomers along a B_{2g} symmetry coordinate.

[e] This value is for the product with C_{2h} symmetry.

[f] See text.

[g] Ref. 44.

ature where it was measured. The results in Table VIII indicate several important points:

1. In every case where a compound is known to exist, its formation reaction is computed to be exothermic.
2. In every case where a compound is known not to exist, its formation reaction enthalpy is computed to be endothermic or very close to zero.
3. For those cases where reaction enthalpies are known, the method described above for computing the enthalpy yields values in excellent agreement with the experimental enthalpies.

The enthalpies for the formation of Al_2Cl_6 and Al_2F_6 computed by this MP2/6−311 + $G(d)$//RHF/6−311 + $g(d)$ method are in slightly better agreement with experimental values than the MP2/6−31$g(d)$//RHF/6−31$g(d)$ values reported recently by Bock et al.[5e] While no experimental data exists for the gas phase enthalpies of formation of the ions in Table VIII, the results discussed previously for the effects of basis set size and electron correlation on the formation of BF_4^- play a role here as well. Those results suggest that the ion formation enthalpies reported in Table VIII are at worst within about 10 kJ/mol of their converged values. The data in Table VIII also strongly suggest that the previously unknown $B_2Cl_7^-$ is energetically stable and hence can be discovered in appropriate experiments. It is important to note that the formation of $B_2Cl_7^-$ is calculated to be exothermic by considerably more than 10 kJ/mol. It is also important to note that the computed formation enthalpy for $B_2Cl_7^-$ is smaller in magnitude than that for the valence isoelectronic species $Al_2Cl_7^-$, $Al_2F_7^-$, and $B_2F_7^-$. The relatively small and exothermic enthalpy of formation for $B_2Cl_7^-$ is consistent with a species that would readily dissociate at room temperature and thus would be a likely candidate for an intermediate in an exchange reaction.

Gilbert et al.[6] used Raman spectroscopy to study several fluoride containing chloroaluminate melts. They found four vibrational frequencies in acidic melts of this type that were due to a new species. They concluded, from the polarization of the Ra-

man bands and an approximate normal mode analysis, that this species was $Al_2Cl_6F^-$ and not Al_2Cl_6F, with the fluorine substituted at one of the terminal positions. The result in Table VIII are consistent with this conclusion in the sense that the formation of the substituted anion is calculated to be energetically favored over the formation of the substituted neutral compound. The computed reaction enthalpies do suggest, however, that the formation of a product with the fluorine in the bridging position is more favorable than formation of a species with a terminal fluorine atom; this is the opposite of what was concluded from measured spectra. This discrepancy suggests that kinetic factors, which are entirely neglected in the computations, play an important role in determining the site at which a fluoride ion will add to the aluminum chloride dimer.

Structures

The details of the structures computed at the RHF/6–311 + $g(d)$ are given in Table II. For those cases where an experimental structure is available, the agreement between the computed structures with the experimental ones is generally good. The bond length errors are typically less than about 0.03 Å. The agreement is somewhat better for the neutrals than for the anions. The structures are computed in the gas phase and it is only for the neutrals that gas phase experimental structures exist. Gas phase structures are not known for any of the anions in this study. Thus the experimental structural data for anions in Table II come from crystallographic studies of salts. Crystal packing effects may be expected to perturb the anion structures. These effects are not well modeled by *ab initio* methods.

Higher levels of theory were used to gauge these packing effects. Rather than only compare a computed anion structure to a measured crystal structure, we also attempted to find an "ideal" gas phase anion structure: one in which the structure was optimized at a rather high level of theory. This was attempted for tetrafluoroborate, using larger basis sets at the MP2 level, or the 6–311 + $g(d)$ basis set at the QCISD levels. These correlated methods were used because they are the highest levels in Gaussian 92 for which analytic derivatives are available. The results are presented in Table IV. The results show that at the MP2 level of theory, the converged bond length is 1.406 Å. The QCISD optimization gives a somewhat longer bond length. Hence an "ideal" *ab initio* bond length for this anion is perhaps 1.41 Å, which is slightly shorter than the solid state value of 1.43 Å.[37] The RHF/6–311 + $g(d)$ value is 1.395 Å; thus the length at this level is about 0.02 Å shorter than the ideal gas phase bond length. Hence the bond lengths computed with this method may also be within a few hundredths of an Ångstrom from their ideal gas phase values as well.

Some of the species in this study have sufficient symmetry that only a few parameters are required to find a fully optimized structure. Al_2Cl_6 and Al_2F_6 are such species. For these, and a few others, optimizations were also carried out at the MP2/6–311 + $g(d)$ level. The structure for Al_2Cl_6 computed at this level is in excellent agreement with the experiment. Bond lengths differ by less than 0.01 Å, and bond angles by less than 0.4°.[22] The accuracy of this method should be similar for Al_2F_6, so the structural parameters in Table II for this species (whose gas phase structure is not known from experiment) should be quite good.

The previously unknown $B_2Cl_7^-$ should have a structure similar to that given in Table II. $B_2Cl_7^-$ consists of two approximately tetrahedral BCl_4 units sharing a single Cl atom with a strongly bent B-Cl-B linkage; this species has no symmetry. $Al_2F_7^-$ is similar except the Al-F-Al linkage is linear and the two tetrahedral units are staggered, giving a structure with D_{3d} symmetry. This is consistent with the suggestion of Gilbert et al. that such an Al-F-Al bridge would very likely be linear.[6]

All of the structures summarized in Table II have computed vibrational frequencies that are listed in the Appendix. There are some points associated with these frequencies that should be noted. All of the frequencies for all of the species are positive real numbers except for one. Thus, all of the structures represent energy minima with the exception of B_2F_6, which has one significant (235 cm^{-1} in magnitude) pure imaginary frequency in D_{2h} symmetry and 14 cm^{-1} in C_{2h}. The magnitude of this frequency is sufficiently large so that it is unlikely that the corresponding negative Hessian eigenvalue is negative only due to cumulative rounding and truncation errors. Thus this species is a transition state. The mode associated with this frequency can be visualized as a dissociation into BF_3 monomers. It has been suggested[26] that a D_{2h} symmetry transition state might be involved in the known rapid exchange of halogens in the boron trihalide mixtures; the transition state nature of B_2F_6 is entirely consistent with this suggestion.

It is well known that vibrational frequencies computed at the HF level are generally about 10%

higher than the experimental frequencies.[35] This is due in part to the neglect of electron correlation in the HF calculation and in part to the assumption of perfectly harmonic vibrational motion in the frequency calculation. Hence it is quite interesting that the E and one of the T_2 modes for AlF_4^- have computed frequencies *below* the measured frequency. It is quite unlikely that there is any confusion on the assignment of either the computed or the experimental frequencies for an anion this simple and with such high symmetry.

It is also worth noting that for Al_2Cl_6 and Al_2F_6, two species for which very high quality experimental vibrational data exist,[38,39] there are some discrepancies between the symmetry species of the computed and experimentally assigned normal modes. The differences are more pronounced for Al_2Cl_6 because the experimental work in this case was of sufficient detail and quality to assign many of the modes. The assignments in the Appendix for Al_2Cl_6 are those of Tomita et al.[38] The computed frequency closest to the assigned one is listed in the table, even when the calculation indicates that the mode has a different symmetry type. In no case do the calculations and experimental assignments differ on whether a mode is of "g" or "u" type. Also, Tomita et al. suggested from their normal coordinate analysis that ν_5, an A_u mode that they did not observe, should have a frequency of 55 cm^{-1} and should be a pure bending mode of the terminal Cl-Al-Cl bond angles. Our calculations put this frequency at 68 cm^{-1} and show that it is indeed a pure bending mode of these terminal angles.

In summary, the Raman spectra of these acidic melts indicate the presence of significant amounts of BCl_3, while the NMR spectra show no evidence for the presence of this species; this suggests an exchange reaction. The DISPA results indicate that the exchange rate must be very high, and the acidic character of these melts indicates that the exchange intermediate is $B_2Cl_7^-$. The MO calculations indicate that the latter species should be stable. These calculations also correctly indicate that the related anions $B_2F_7^-$, $Al_2F_7^-$, and $Al_2Cl_7^-$ are stable. The calculations also correctly predict the stability of the species studied that are known to be stable; they correctly predict the instability of the species known not to be stable. Hence we conclude that $B_2Cl_7^-$ is probably present in the acidic tetrachloroborate melts, as an intermediate in the exchange reaction. It is likely that the formation of $B_2Cl_7^-$ from BCl_3 and BCl_4^- is the principle cause of the unexpected negative entropy of solution for boron trichloride dissolving in the acidic melt. This entropy loss may be related to the much lower symmetry of the $B_2Cl_7^-$ dimer compared to the high symmetry of the BCl_3 and BCl_4^- monomers.

Conclusions

The *ab initio* MO calculations described here appear to do a fairly good job of predicting stabilities and formation reaction enthalpies for neutral and anionic aluminum and boron fluorides and chlorides. Computed structures and vibrational frequencies are in good agreement with experimental values. The calculations predict that the previously unknown $B_2Cl_7^-$ should be stable. Raman and ^{11}B NMR spectroscopy of some room temperature tetrachloroborate melts suggest that $B_2Cl_7^-$ is present in these melts as an intermediate in an exchange reaction.

Acknowledgments

This work was supported in part by Grant 88-0307 from the Air Force Office of Scientific Research. We would like to thank the Microelectronics Center for North Carolina (MCNC) for providing computer time for the *ab initio* calculations.

Appendix: Vibrational Frequencies

Frequencies are computed at the RHF/6–311 + $G(d)$//RHF/6–311 + $G(d)$ level. Experimental values are given in brackets. Frequencies are given in cm^{-1}.

$AlCl_3$: E': 154, [148]; A_2'': 213, [214]; A_1': 401, [375]; E': 642, [616]; ref. 38.

$AlCl_4^-$: E: 121, [119]; T_2: 187, [182]; A_1: 355, [348]; T_2: 508, [498]; ref. 45.

Al_2Cl_6: B_{2u}: 23; A_u: 68; A_g: 101, [98]; B_{1g}: 124, [105]†,‡; B_{3g}: 126, [115] †; B_{1u}: 138, [123]†; B_{3u}: 146, [143]; B_{2g}: 176, [168]†; B_{2u}: 190, [178]†; A_g: 233, [219]†; B_{2g}: 272, [281]†; B_{3u}: 332, [320]; A_g: 354, [337]†; B_{1u}: 429, [418]†; B_{3u}: 496, [483]; A_g: 537, [511]; B_{1g}: 635, [614]†; B_{2u}: 646, [626]†; ref. 38.

$Al_2Cl_7^-$: 14; 18; 40; 91; 91; 99, [112]; 125; 151, [152]; 162; 167; 182, [176]; 196; 207, [226]; 312, [310]; 337, [336]; 395, [383]; 442, [429]; 550, [526]; 554, [540]; 570, [550]; 570, [560]; ref. 46.

AlF_3: E': 251, [270]; A_2'': 310, [300]; A_1': 722; E': 1001, [965]; ref. 39.

AlF_4^-: E: 205, [210]; T_2: 318, [322]; A_1: 642, [622]; T_2: 821, [760]; ref. 47.

Al_2F_6: B_{2u}: 61; A_u: 98; B_{1g}: 167; A_g: 173; B_{3g}: 206; B_{1u}: 218; B_{3u}: 228, [300][†]; B_{2g}: 270; B_{2u}: 346, [340]; A_g: 415; B_{2g}: 470; B_{3u} 590, [575]; B_{1u}: 598, [600][†]; A_g: 626; B_{3u}: 820, [805][†]; A_g: 869; B_{1g}: 1007; B_{2u}: 1025, [995][†]; ref. 39.

$Al_2F_7^-$: A_{1u}: 19; E_u: 41; E_g: 147; A_{1g}: 179; E_u: 217; E_g: 272; A_{2u}: 315; E_u: 330; A_{1g}: 469; A_{2u}: 689; A_{2u}: 732; A_{1g}: 737; E_g: 885; E_u: 897.

BCl_3: E': 271, [254]; A_2'': 480, [447]; A_1': 491, [473]: E': 996, [951]; ref. 48.

BCl_4^-: E: 196, [188]; T_2: 286, [273]; A_1: 419, [405]; T_2: 721, [696]; ref. 11.

B_2Cl_6: B_{2u}: 19; B_{2g}: 75; A_u: 122; A_g: 162; B_{1u}: 211; B_{3g}: 213; B_{1g}: 227; B_{3u}: 255; B_{2u}: 302; B_{2g}: 341; A_g: 346; B_{3u}: 396; A_g: 407; B_{1u}: 619; B_{3u}: 666; A_g: 774; B_{1g}: 939; B_{2u}: 957.

$B_2Cl_7^-$: 24; 38; 67; 104; 134; 151; 201; 205; 236; 273; 279; 286; 322; 337; 396; 473; 569; 806; 821; 846; 849.

BF_3: E': 506, [482]; A_2'': 774, [718]; A_1': 931, [888]; E': 1577, [1505]; ref. 49.[§]

BF_4^-: E: 368, [360]; T_2: 541, [533]; A_1: 794, [777]; T_2: 1123, [1070]; ref. 50.

B_2F_6: B_{2g}: 235i; B_{2u}: 76; A_u: 208; A_g: 303; B_{1u}: 370; B_{3g}: 380; B_{1g}: 381; B_{3u}: 470; B_{2u}: 554; B_{2g}: 589; A_g: 665; B_{3u}: 685; A_g: 752; B_{1u}: 911; B_{3u}: 1090; A_g: 1260; B_{1g}: 1515; B_{2u}: 1565 (for D_{2h} geometry).

B_2F_6: B_u: 14i; A_u: 17; A_u: 32; B_g: 33; A_g: 35; A_g: 122; B_g: 499; B_u: 503; A_g: 504; A_u: 507; B_u: 730; A_g: 737; A_g: 927; B_u: 929; A_g: 1501; B_u: 1503; B_g: 1525; A_u: 1542 (for C_{2h} geometry).

$B_2F_7^-$: 25; 32; 75; 249; 267; 277; 380; 417; 417; 461; 508; 527; 538; 561; 616; 732; 874; 982; 1263; 1267; 1302; 1308.

Al_2Cl_5F, bridging F: B_1: 34; A_2: 63; A_1: 106; A_2: 126; A_1: 141; B_1: 142; B_2: 147; B_2: 194; B_1: 267; B_2: 276; A_1: 278, [311]; A_1: 396, [393]; B_2: 454, [437]; A_1: 501, [489]; B_2: 594; A_1: 614; A_2: 643; B_1: 663; ref. 6.[‖]

Al_2Cl_5F, terminal F: A': 26; A'': 76; A': 109; A'': 126; A': 132; A'': 153; A': 167; A'': 198; A': 201; A': 251; A'': 278; A': 340; A': 369; A'': 441; A': 512; A': 577; A': 642; A': 912.

$Al_2Cl_6F^-$, bridging F: A_{1u}: 12; E_u: 33; E_g: 94; A_{1g}: 110; E_u: 143; E_g: 171; A_{2u}: 206; E_u: 270; A_{1g}: 330; A_{2u}: 399; A_{1g}: 504; E_g: 555; E_u: 572; A_{2u}: 679.

$Al_2Cl_6F^-$, terminal F: 13; 18; 40; 92; 99; 103; 132; 160; 170; 184; 192; 218; 232; 325, [311]; 346, [393]; 411, [437]; 463, [489]; 551; 563; 573; 854; ref. 6.[‖]

[†] The assignment of this frequency differs between the calculation and the reference. In no case do the calculations differ on "g" or "u" type modes from the reference.

[‡] This frequency was assumed rather than measured in the reference.

[§] The experimental frequencies are for the boron-10 isotopomer; the computed frequencies reported here are for this isotopomer as well, but the frequencies and zero point energies used elsewhere in this article are for the more common boron-11 species (which are 504, 744, 931, and 1521).

[‖] Four polarized Raman bands were observed at 311, 393, 437, and 489 cm^{-1} for the product of a reaction between Al_2Cl_6 and NaF; these were attributed to $Al_2Cl_6F^-$ with a terminal fluorine atom. These frequencies seem to match the frequencies of Al_2Cl_5F with a bridging fluorine atom somewhat better. The association with Al_2Cl_5F also implies that the observed mode at 437 cm^{-1} is of B_2 symmetry and should be depolarized. Because this band is clearly polarized in the Raman spectrum, these bands should not be associated with Al_2Cl_5F.

References

1. G. A. Olah, Ed., *Friedel-Crafts and Related Reactions*, Wiley, New York, 1963.
2. (a) G. Mamantov and R. Marassi, Eds., *Molten Salt Chemistry: An Introduction and Selected Applications*, Proceedings of the NATO Advanced Study Institute on Molten Salt Chemistry, Reidel Publishing Company, Dordrecht, 1987; (b) G. Mamantov and R. A. Osteryoung, In *Characterization of Solutes in Non-Aqueous Solvents*, G. Mamantov, Ed., Plenum Press, New York, 1978, p. 223.
3. (a) C. Leibovici, *J. Mol. Struct.*, **14**, 459 (1972); (b) M. Blander, E. Bierwagen, K. G. Calkins, L. A. Curtiss, D. L. Price, and M. L. Saboungi, *J. Chem. Phys.*, **97**, 2733 (1993).
4. (a) G. L. Gutsev and A. I. Boldyrev, *Chem. Phys. Lett.*, **84**, 352 (1981); (b) J. A. Tossel, *Physica*, **131B**, 283 (1985); (c) G. L. Gutsev and A. I. Boldyrev, *J. Struct. Chem.*, **25**, 678 (1984).
5. (a) D. S. Marynick, L. Throckmorton, and R. Bacquet, *J. Am. Chem. Soc.*, **104**, 1 (1982); (b) S. C. Choi, R. J. Boyd, and O. Knop, *Can. J. Chem.*, **66**, 2465 (1988); (c) G. Gutsev, A. Les, and L. Adamowicz, *J. Chem. Phys.*, **100**, 8925 (1994); (d) P. G. Jasien, *J. Phys. Chem.*, **96**, 9273 (1992); (e) C. W. Bock, M. Trachtman, and G. J. Mains, *J. Phys. Chem.*, **97**, 2546 (1993); (f) C. W. Bock, M. Trachtman, and G. J. Mains, *J. Phys. Chem.*, **98**, 478 (1994); (g) J. H. Francisco and I. H. Williams, *J. Phys. Chem.*, **90**, 8522 (1990); (h) M. Spoliti, N. Sanna, and V. Di Martino, *J. Mol. Struct.: Theochem.*, **285**, 83 (1992); (i) V. G. Zakzhevskii, A. I. Boldyrev, and O. P. Charkin, *Russ. J. Inorg. Chem.*, **25**, 651 (1980); (j) L. M. Nxumalo and T. A. Ford, *J. Mol. Struct.*, **300**, 325 (1993); (k) H. Horn and R. Ahlrichs, *J. Am. Chem. Soc.*, **112**, 2121 (1990); (l) F. M. M. O'Neill, G. A. Yeo, and T. A. Ford, *J. Mol. Struct.*, **173**, 337 (1988); (m) L. A. Curtiss, In *Proceedings of the Joint International Symposium on Molten Salts*, G. Mamantov, Ed., The Electrochemical Society, Pennington, NJ, 1987. p. 185.

6. B. Gilbert, S. D. Williams, and G. Mamantov, *Inorg. Chem.*, **27**, 2359 (1988).
7. C. L. Hussey, In *Advances in Molten Salt Chemistry*, Vol. 5, G. Mamantov, Ed., Elsevier, New York, 1983, p. 185.
8. C. F. Poole, B. R. Kersten, S. S. J. Ho, M. E. Coddens, and K. C. Furton, *J. Chromatogr.*, **352**, 407 (1986).
9. S. P. Wicelinski, R. J. Gale, S. D. Williams, and G. Mamantov, *Spectrochim. Acta*, **45A**, 759 (1989).
10. M. G. De Backer, E. B. Mkadmi, F. X. Sauvage, J. P. Lelieur, M. J. Wagner, R. Concepcion, J. L. Eglin, R. A. Gaudagnini, J. Kim, L. E. H. McMillis, and J. L. Dye, *J. Am. Chem. Soc.*, **116**, 6570 (1994).
11. S. D. Williams, J. P. Schoebrechts, J. C. Selkirk, and G. Mamantov, *J. Am. Chem. Soc.*, **109**, 2218 (1987).
12. G. Torsi, G. Mamantov, and G. M. Begun, *Inorg. Nucl. Chem. Lett.*, **6**, 533 (1970).
13. S. J. Cyvine, P. K. Klaboe, E. Rytter, and H. A. Oye, *J. Chem. Phys.*, **52**, 2776 (1970).
14. J. S. Hartman, and P. Stilbs, *J. Chem. Soc. Chem. Commun.*, 566 (1975).
15. H. Nöth and B. Wrackmeyer, In *NMR Basic Principles and Progress, Nuclear Magnetic Resonance Spectroscopy of Boron Compounds*, Vol. 14, P. Diehl, E. Fluck, and R. Kosfeld, Eds., Springer–Verlag, New York, 1978.
16. W. D. Phillips, H. C. Miller, and E. L. Muetterties, *J. Am. Chem. Soc.*, **81**, 4496 (1959). (The shift values from this work have been converted to the equivalent BF_3 etherate reference values before reporting them here.)
17. H. Landesman and R. E. Williams, *J. Am. Chem. Soc.*, **83**, 2663 (1961).
18. R. K. Harris, A. Root, and K. B. Dillon, *Spectrochim. Acta*, **39A**, 309 (1983).
19. R. Balz, U. Brandle, E. Kammerer, D. Kohnlein, A. Nolle, R. Schafitel, and E. Z. Veil, *Z. Naturforsch.*, **41a**, 737 (1986).
20. J. W. Akitt, *J. Chem. Soc. Faraday Trans. I*, **71**, 1557 (1975).
21. (a) *Gaussian 92, Revision C*, M. J. Frisch, G. W. Trucks, M. Head–Gordon, P. M. W. Gill, M. W. Wong, J. B. Foresman, B. G. Johnson, H. B. Schlegal, M. A. Robb, E. S. Replogle, R. Gomperts, J. L. Andres, K. Raghavachari, J. S. Binkley, C. Gonzalez, R. L. Martin, D. J. Fox, D. J. Defrees, J. Baker, J. J. P. Stewart, and J. A. Pople, Gaussian, Inc., Pittsburgh, PA, 1992; (b) *Gaussian 94, Revision B.3*, M. J. Frische, G. W. Trucks, H. B. Schlegel, P. M. W. Gill, B. G. Johnson, M. A. Robb, J. R. Cheeseman, T. Keith, G. A. Petersson, J. A. Montgomery, K. Raghavachari, M. A. Al-Laham, V. G. Zakrzewski, J. V. Ortiz, J. B. Foresman, C. Y. Peng, P. Y. Ayala, W. Chen, M. W. Wong, J. L. Andres, E. S. Replogle, R. Gomperts, R. L. Martin, D. J. Fox, J. S. Binkley, D. J. Defrees, J. Baker, J. P. Stewart, M. Head–Gordon, C. Gonzalez, and J. A. Pople, Gaussian, Inc., Pittsburgh, PA, 1995.
22. T. W. Couch, D. A. Lokken, and J. D. Corbett, *Inorg. Chem.*, **11**, 357 (1972).
23. (a) L. Onsager, *J. Am. Chem. Soc.*, **58**, 1486 (1936); (b) M. W. Wong, M. J. Frisch, and K. B. Wiberg, *J. Am. Chem. Soc.*, **113**, 4776 (1991).
24. Q. Shen, Ph.D. thesis, Oregon State Univ., Corvallis, OR, 1974.
25. R. F. Porter and E. E. Zeller, *J. Chem. Phys.*, **33**, 858 (1960).
26. F. A. Cotton and G. Wilkinson, *Advanced Inorganic Chemistry, A Comprehensive Text*, Wiley, New York, 1972.
27. A. Loewenschuss, *Spectrochim. Acta*, **31A**, 679 (1975).
28. H. G. M. Edwards, V. Fawcett, and G. P. J. Price, *J. Mol. Struct.*, **220**, 227 (1990).
29. (a) J. M. Bassler, P. L. Timms, and J. L. Margrave, *J. Chem. Phys.*, **45**, 2704 (1966); (b) I. W. Levin and S. Abromowitz, *Chem. Phys. Lett.*, **9**, 247 (1971); (c) J. Gebicki and J. Lang, *J. Mol. Struct.*, **117**, 283 (1984).
30. S. J. Hartmen and G. J. Schrobilgen, *Inorg. Chem.*, **11**, 940 (1972).
31. R. J. Thompson and J. C. Davis, *Inorg. Chem.*, **4**, 1464 (1965).
32. J. A. Dean, Ed., *Lange's Handbook of Chemistry*, McGraw–Hill, New York, 1973.
33. (a) A. G. Marshall, In *Fourier, Hadamard, and Hilbert Transforms in Chemistry*, A. G. Marshall, Ed., Plenum, New York, 1982, p. 99; (b) A. G. Marshall and R. E. Bruce, *J. Magn. Reson.*, **39**, 47 (1980).
34. K. B. Dillon and G. F. Hewitson, *Polyhedron.*, **3**, 957 (1984).
35. W. J. Hehre, L. Radom, P. v. R. Schleyer, and J. A. Pople, *Ab Initio Molecular Orbital Theory*, Wiley, New York, 1986.
36. (a) E. U. Wurthwein, M. B. Krogh–Jespersen, and P. v. R. Schleyer, *Inorg. Chem.*, **20**, 3663 (1981); (b) A. I. Boldyrev and O. P. Charkin, *Russ. J. Coord. Chem.*, **8**, 331 (1982).
37. R. W. G. Wyckoff, *Crystal Structures*, 2nd ed., Vol. 3, Wiley, New York, 1965.
38. T. Tomita, C. E. Sjøgren, P. Klaeboe, G. N. Papatheodorou, and E. Rytter, *J. Raman Spectrosc.*, **14**, 415 (1983).
39. A. Snelson, *J. Phys. Chem.*, **71**, 3202 (1967).
40. V. P. Spiridonov, A. G. Gershikov, E. Z. Zasorin, N. I. Popenko, and L. I. Ermolayeva, *High Temp. Sci.*, **14** 285 (1981).
41. (a) G. V. Girichev, A. N. Utkin, and N. I. Giricheva, *Izv. Vyssh, Uchebn. Zaved. Khim. Khim. Tekhnol.*, **26**, 634 (1983); (b) M. W. Chase, Jr., C. A. Davis, J. R. Downey, Jr., D. J. Frurip, R. A. McDonald, and A. N. Syverud, *JANAF Thermochemical Tables*, 3rd ed., Plenum, New York, 1985.
42. A. F. Wells, *Structural Inorganic Chemistry*, 5th ed., Clarendon Press, Oxford, 1984.
43. A. Koblischek, H. D. Hausen, J. Weidlein, and H. Binder, *Z. Naturforsch.*, **38b**, 1046 (1983).
44. G. L. Sidorov, M. I. Nikiten, E. V. Skokan, and I. D. Sorokin, *Int. J. Mass Spectrom. Ion Phys.*, **35**, 203 (1980).
45. E. Rytter and H. A. Øye, *J. Inorg. Nucl. Chem.*, **35**, 4311 (1973).
46. A. Manteghetti and A. Potier, *Spectrochim. Acta*, **38A**, 141 (1982).
47. B. Gilbert, G. Mamantov, and G. M. Begun, *Inorg. Nucl. Chem. Lett.*, **10**, 1123 (1974).
48. (a) R. H. J. Clark and P. D. Mitchell, *J. Chem. Phys.*, **56**, 2225 (1972); (b) D. A. Downs and G. Bottger, *J. Chem. Phys.*, **34**, 689 (1961).
49. J. Vanderryn, *J. Chem. Phys.*, **30**, 331 (1959); D. A. Downs, *J. Chem. Phys.*, **31**, 1637 (1959).
50. A. S. Quist, J. B. Bates, and G. E. Boyd, *J. Chem. Phys.*, **54**, 4896 (1971).